**The EMBO Journal (2006) 25,** 5180–5190 | © 2006 European Molecular Biology Organization | All Rights Reserved 0261-4189/06
www.embojournal.org

THE EMBO JOURNAL

# POT1b protects telomeres from end-to-end chromosomal fusions and aberrant homologous recombination

**Hua He[1,4], Asha S Multani[1,4], Wilfredo Cosme-Blanco[1], Hidetoshi Tahara[2], Jin Ma[1], Sen Pathak[1], Yibin Deng[1] and Sandy Chang[1,3,*]**

[1]Department of Molecular Genetics, The University of Texas MD Anderson Cancer Center, Houston, TX, USA, [2]Department of Cellular and Molecular Biology, Program for Biomedical Research, Graduate School of Biomedical Sciences, Hiroshima University, Minami-ku, Hiroshima, Japan and [3]Department of Hematopathology, The University of Texas MD Anderson Cancer Center, Houston, TX, USA

**POT1 (protection of telomere 1) is a highly conserved single-stranded telomeric binding protein that is essential for telomere end protection. Here, we report the cloning and characterization of a second member of the mouse POT family. POT1b binds telomeric DNA via conserved DNA binding oligonucleotide/oligosaccharide (OB) folds. Compared to POT1a, POT1b OB-folds possess less sequence specificity for telomeres. In contrast to POT1a, truncated POT1b possessing only the OB-folds can efficiently localize to telomeres *in vivo*. Overexpression of a mutant *Pot1b* allele that cannot bind telomeric DNA initiated a DNA damage response at telomeres that led to p53-dependent senescence. Furthermore, a reduction of the 3′ G-rich overhang, increased chromosomal fusions and elevated homologous recombination (HR) were observed at telomeres. shRNA mediated depletion of endogenous *Pot1b* in *Pot1a* deficient cells resulted in increased chromosomal aberrations. Our results indicate that POT1b plays important protective functions at telomeres and that proper maintenance of chromosomal stability requires both POT proteins.**

*The EMBO Journal* (2006) **25,** 5180–5190. doi:10.1038/sj.emboj.7601294; Published online 19 October 2006
*Subject Categories*: genome stability & dynamics
*Keywords*: genomic instability; POT1b; telomere; telomerase

## Introduction

Telomeres are specialized protein–DNA complexes that cap the ends of linear chromosomes and maintain genome stability by providing both end protection and a mechanism for complete replication of chromosomal termini. In mammals, telomeres consist of TTAGGG repetitive sequences that terminate in single-stranded (ss) 3′ G-rich overhangs that can be sequestered into lariat-like structures termed the t-loop (Griffith *et al*, 1999; Murti and Prescott, 1999; Nikitina and Woodcock, 2004). A model has been proposed in which this altered telomeric conformation is required to protect telomeres from being recognized as double-stranded DNA breaks (DSBs) that would otherwise activate DNA damage checkpoint responses (reviewed in de Lange, 2005). Failure to properly maintain telomere end capping functions results in dysfunctional telomeres that are processed by the DNA damage response pathways to initiate the onset of replicative senescence or fuel genomic instability associated with cancer cells (Karlseder *et al*, 1999; Celli and de Lange, 2005; Wong *et al*, 2006).

The telomeric G-rich overhang is evolutionarily conserved and is a substrate for ss DNA binding proteins TEBPαβ (telomere end binding protein) found in the ciliate *Oxytricha nova* (Price and Cech, 1987), Cdc13p from *Saccharomyces cerevisiae* (Garvik *et al*, 1996; Chandra *et al*, 2001) and protection of telomere 1 (POT1), first identified in *S. pombe* and are present in diverse organisms including plant, chicken, mouse and human (Baumann and Cech, 2001; Baumann *et al*, 2002; Wei and Price, 2004; Shakirov *et al*, 2005; Wu *et al*, 2006). All three proteins bind ss telomeric DNA through oligosaccharide/oligonucleotide binding motifs (OB-fold), a structurally conserved protein domain capable of binding to ss DNA with both high affinity and specificity (Mitton-Fry *et al*, 2002; Lei *et al*, 2003, 2004). While POT1, Cdc13p and TEBPαβ all use OB-folds to bind ss telomeric DNA, considerable diversity exists between the DNA binding domains of these proteins. Cdc13p uses only one OB-fold to bind DNA, while POT1 and TEBPαβ use two or more OB-folds for DNA binding (Price and Cech, 1987; Horvath *et al*, 1998; Lei *et al*, 2002, 2004; Trujillo *et al*, 2005). The importance of POT1 in mediating telomere end protection is further revealed by observations that deletion of SpPot1 results in catastrophic loss of telomeric DNA and cell death (Baumann and Cech, 2001). Survivors emerge with circularized chromosomes, obviating the need for the telomeric protective function of *Pot1a*. In addition, conditional knockout of the mouse *Pot1a* gene leads to chromosomal fusions and initiation of replicative senescence (Wu *et al*, 2006). These results indicate that POT1 is an integral telomere end protection protein, and that loss of POT1 results in dysfunctional telomeres that are targeted for chromosomal end-joining reactions.

POT1 is part of a complex of six core telomere-binding proteins termed the telosome (Liu *et al*, 2004b) or shelterin (de Lange, 2005). Both human and mouse POT1 interacts with the TPP1 protein through its C-terminal domain, which in turn interacts with the protein TIN2 (Kim *et al*, 2004; Liu *et al*, 2004a, b; Ye *et al*, 2004a, b; Wu *et al*, 2006). This protein complex can then interact with TRF1 or TRF2/Rap1 to form subcomplexes, although additional studies are required to determine the specific stochiometry of protein subunits (Kim *et al*, 2004; Liu *et al*, 2004b; Ye *et al*, 2004b; Yang *et al*, 2005).

*Corresponding author. Department of Molecular Genetics, The University of Texas MD Anderson Cancer Center, 1515 Holcombe Blvd, Box 1006, Houston, TX 77030, USA. Tel.: +1 713 834 6361; Fax: +1 713 834 6319; E-mail: schang@mdanderson.org
[4]These authors contributed equally to this work

**Received: 27 April 2006; accepted: 24 July 2006; published online: 19 October 2006**

 

As the only ss telomere binding protein in the complex, POT1 serves a critically important role by transducing telomere length information to the TRF1 complex (Loayza and de Lange, 2003). Indeed, reduction of endogenous POT1 levels by siRNA knockdown (Liu *et al*, 2004a; Ye *et al*, 2004a) or elimination of POT1 protein by a conditional knockout approach (Wu *et al*, 2006) results in telomere length elongation. In addition, biochemical analyses using purified POT1 and telomerase demonstrated that POT1 negatively regulates telomerase activity *in vitro* by limiting its access to the terminal G residue of telomeres (Kelleher *et al*, 2005; Lei *et al*, 2005). These results are consistent with POT1's function as a negative regulator of telomere length.

Several organisms possess more than one *Pot* gene, and recent data in plants suggest that different POT proteins may perform different functions in telomere maintenance (Shakirov *et al*, 2005). In this study, we report the identification and characterization of POT1b, a second member of the mouse POT family. POT1b is highly homologous to POT1a and efficiently binds telomeric DNA *in vitro* via its conserved OB-folds. However, in contrast to POT1a, a truncated POT1b protein possessing only the OB-folds can efficiently localize to telomeres *in vivo*. Overexpression of a mutant allele of POT1b resulted in a potent DNA damage response at telomeres and the onset of a p53-dependent senescence phenotype. shRNA mediated depletion of *Pot1b* in the setting of *Pot1* deficiency resulted in increased chromosomal aberrations. Our results indicate that POT1b plays important protective functions at telomeres and that proper maintenance of chromosomal stability requires both POT proteins.

## Results

### *Cloning and sequence analysis of mouse Pot1b*

While the human genome contains a single *Pot1* gene, we identified two *Pot1* orthologs in the mouse and rat genomes (Supplementary Figure 1; Wu *et al*, 2006). In this report, we focus on the characterization of mouse *Pot1b*. *Pot1b* encodes a protein 640 amino acids in length, is located on murine chromosome 17 and is highly homologous to mouse *Pot1a* and human *Pot1* (Supplementary Figure 1A). Like POT1a, POT1b also possesses two OB-folds: OB1 is 74% identical to the corresponding regions in human POT1 and mouse POT1a, while OB2 is 73 and 81% identical to the corresponding regions in mouse POT1a and human POT1, respectively (Supplementary Figure 1A). Importantly, aromatic residues required for stacking interactions of telomeric ss DNA residues, including Phe31, Phe62, Tyr89 and Tyr223 (Lei *et al*, 2004), are evolutionarily conserved across mouse, rat and human POT proteins (Supplementary Figure 1B). In addition, the C-terminal portion of POT1b is 71 and 73% identical to the corresponding region in mouse POT1a and human POT1, respectively. RT–PCR analysis revealed that like *Pot1a*, *Pot1b* is ubiquitously expressed, detected in early embryonic stages and in all adult mouse tissues examined (Supplementary Figure 1C).

### *POT1b efficiently binds to 12 bp telomeric DNA*

Biochemical and structural analyses have revealed that the POT1 OB-folds are critical for binding to telomeric substrates i*n vitro* (Baumann and Cech, 2001; Baumann *et al*, 2002; Lei *et al*, 2003, 2004; Loayza and de Lange, 2003; Loayza *et al*, 2004; Wei and Price, 2004; Wu *et al*, 2006). Efficient binding of human POT1 requires ss telomeric DNA of 9–10 nucleotides that included the core telomeric sequence (T)TAGGGTTAG (Loayza *et al*, 2004; Lei *et al*, 2004). To determine the length of ss telomeric DNA substrate required to efficiently bind POT1b, we generated N-terminal Flag-tagged POT1b (POT1b N) containing both OB-folds (residues 1–341; Figure 2A). *Pot1b* N was translated *in vitro,* and electrophoretic mobility shift assays (EMSA) were performed with radiolabeled ss telomeric DNA substrates of 9–13 nucleotides containing the indicated permutations (Figure 1A). While some complex formation was observed when POT1b N was incubated with the 10-nucleotide core telomeric sequence, efficient binding of POT1b N to telomeric DNA required a minimum of 12 nucleotides (Figure 1A). In addition to the 10 bp core sequence, an additional two 5′ G residues greatly promoted binding, while the addition of three 5′ G residues diminished binding by ~50% compared to the optimal 12-mer GGTTAGGGTTAG substrate (Figure 1A).

Crystal structural analysis of both *S. pombe* and human POT1 proteins identified a series of highly conserved aromatic residues within the OB-folds predicted to be important for binding to telomeric sequences (Lei *et al*, 2003, 2004). To test whether these amino-acid residues are required for POT1b binding to ss telomeric DNA, we generated *Pot1b* N constructs containing either wild-type OB-folds or a series of *Pot1b* N mutants possessing specific point mutations within OB1 (Phe62Ala and Tyr89Ala) and OB2 (Tyr223Ala) using site-directed mutagenesis (Figure 2A). Structural and genetic analyses predicted that these mutations should disrupt POT1b binding to ss telomeric DNA (Lei *et al*, 2003). Amino-acid residue Y223 within OB2 is of particular interest, because it is predicted from structural analysis to sequester the terminal G-residue of telomeric DNA, and access of this particular G-residue by telomerase appears to be critical for telomere elongation (Lei *et al*, 2004, 2005; Kelleher *et al*, 2005). EMSA performed with the 12-mer GGTTAGGGTTAG ss telomeric DNA confirmed that POT1a N and POT1b N possessing wild-type OB-folds efficiently bound ss telomeric DNA with similar affinities to form protein–DNA complexes (Figure 1B). In contrast, the F62A and Y223A substitutions within both POT1a N and POT1b N diminished complex formation by ~80% (Figure 1B and data not shown), confirming their importance for binding to ss telomeric DNA. Interestingly, POT1b$^{Y89A}$ N was able to bind ss telomeric DNA at reduced affinity, even though structural analysis predicted that Y89 is important for stacking interactions involving telomeric residues A3 and G4 (Lei *et al*, 2004). Taken together, these results support data from human POT1 crystal structural studies that evolutionarily conserved aromatic residues within the POT1b OB-folds are important for binding to ss telomeric DNA.

To identify nucleotides within the telomeric repeat that is critical for stable interaction with both mouse POT1a and POT1b, a series of 12 nucleotide ss telomeric DNAs containing single-nucleotide substitutions within the core telomeric sequence was evaluated for POT1a N and POT1b N binding via EMSA. Comparison of the mobility shift profiles between these two proteins revealed that POT1a N displayed greater specificity for telomeric sequences (Figures 1C and 2D). POT1b N was able to bind with at least 30% efficiency to almost all of the substituted ss telomeric DNA substrates,

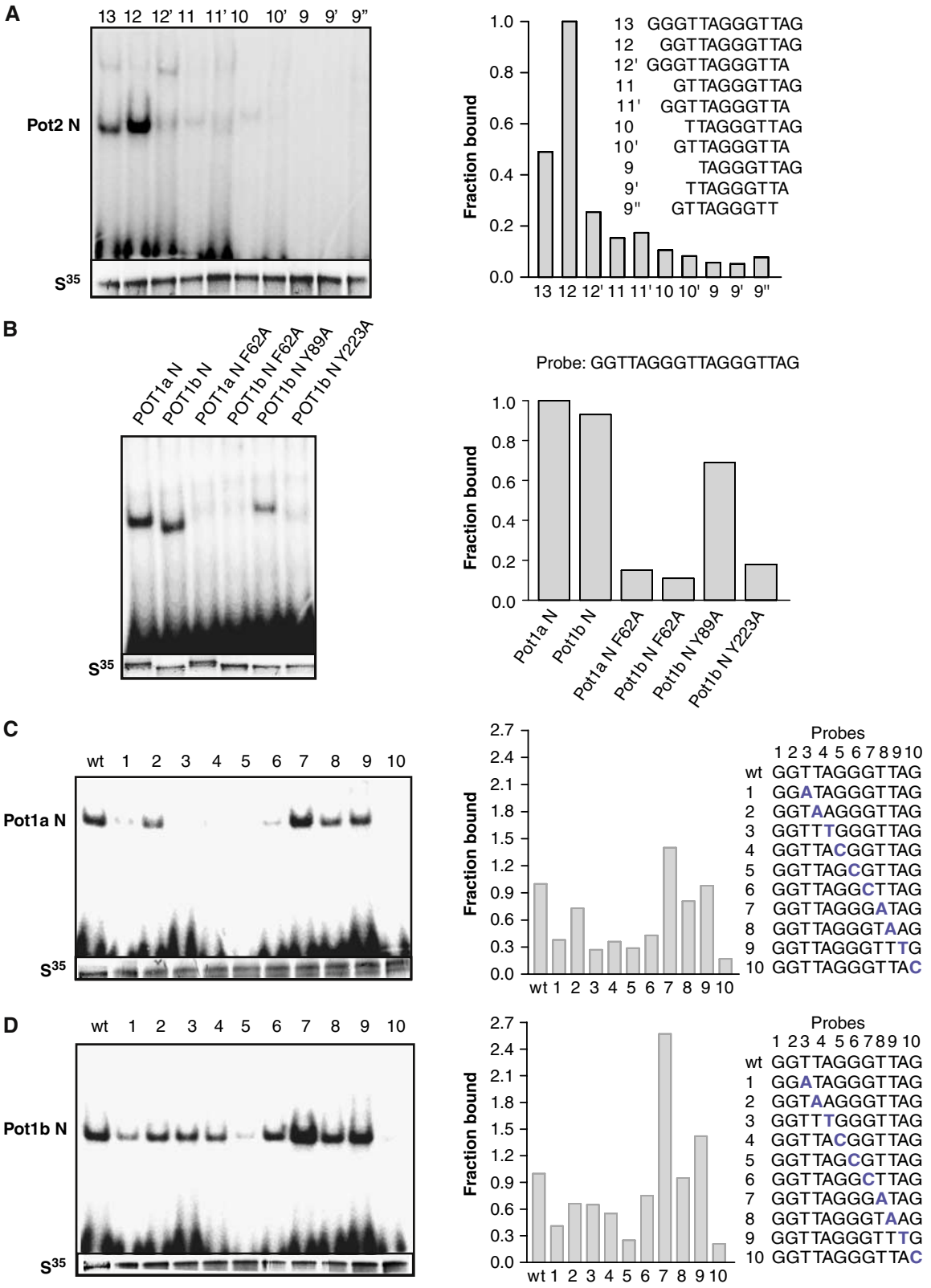


**Figure 1** Characterization of POT1b interaction with ss telomeric DNA *in vitro*. (**A**) POT1b efficiently binds to a 12 base ss telomeric DNA sequence GGTTAGGGTTAG. *In vitro* translated POT1b ($S^{35}$) was incubated with $^{32}$P-labeled telomeric oligonucleotides with the indicated nucleotide permutations and complexes were resolved by native PAGE. The fraction of POT1b bound to various telomeric substrates is plotted on the right, with POT1b binding to the 12-mer telomeric sequence set at 1.0. (**B**) Mutations with the OB-folds abolish POT1a and POT1b binding to ss telomeric DNA. POT1a N and POT1b N constructs bearing wild-type OB-folds or the indicated point mutations were incubated with the12-mer ss telomeric DNA sequence and subjected to gel mobility shift assays. The fraction of complex formed is plotted to the right. (**C**) Specificity of ss telomeric DNA binding to POT1a N and (**D**) POT1b N. Numbers indicate nucleotide position within the 12-base core tight-binding telomeric DNA sequence, in which one nucleotide at a time (in bold) was substituted with its complement. The fraction of complex formed is plotted on the right, with binding to wild-type telomeric sequence set at 1.0.

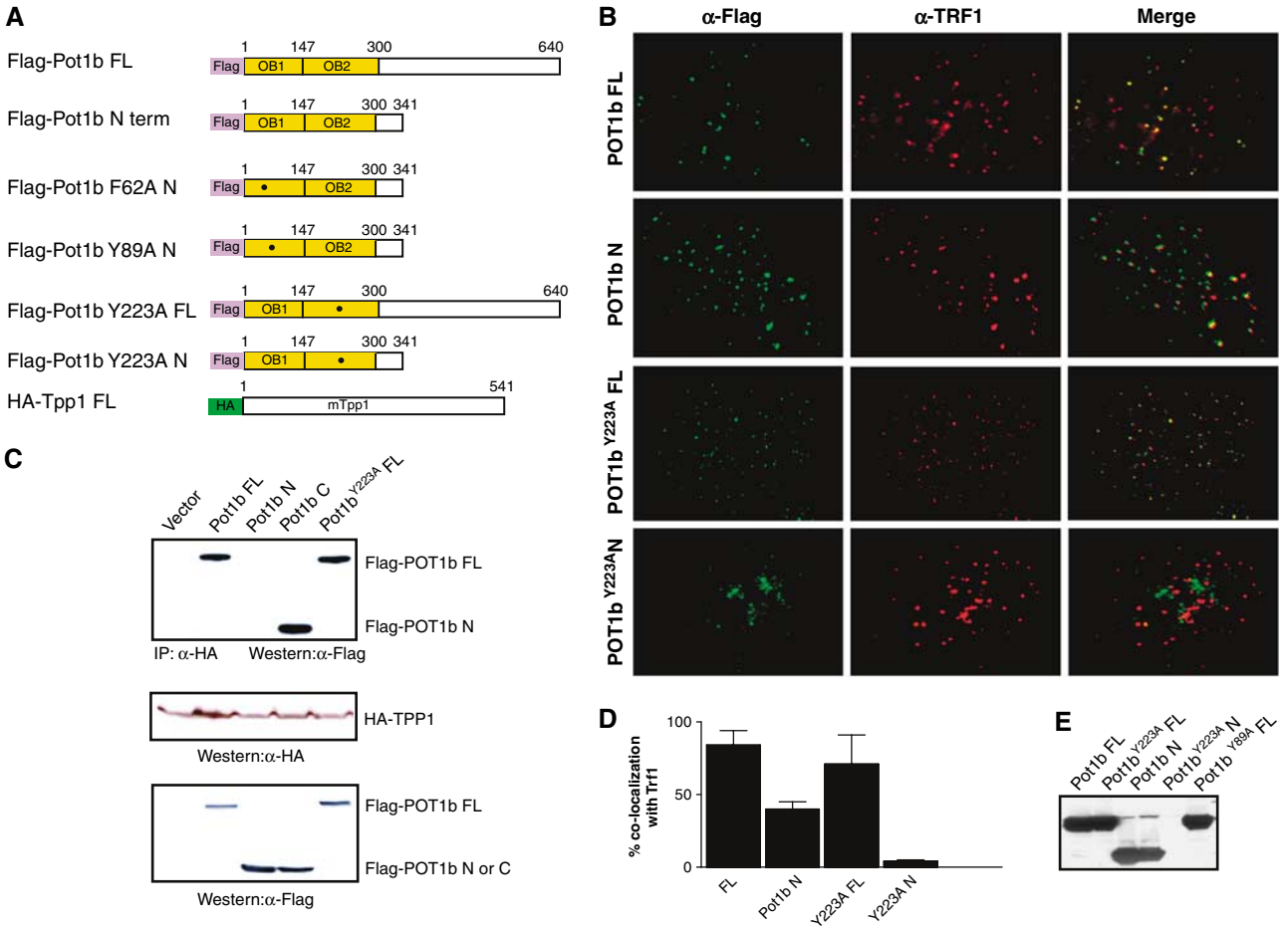


**Figure 2** Biological properties of POT1b. (**A**) Schematic of N-terminal Flag-tagged full-length (FL) POT1B, POT1B N and derivative point mutants. (**B**) Co-localization of Flag-tagged FL POT1B, POUT1B N, FL POT1B$^{Y223A}$ and POT1B$^{Y223A}$ N with TRF1 in p53$^{-/-}$ MEFs. Growing cells were transiently infected with the indicated retroviral constructs, fixed and stained with mouse anti-Flag and rabbit anti-TRF1. Representative images are shown. (**C**) POT1b interacts with TPP1 via its C-terminal domain. Flag-tagged POT1B constructs were transfected into 293 T cells along with HA-tagged TPP1. IP-Western: IP pulldown and Western analysis were performed with the indicated antibodies. Western blots with anti-Flag and anti-HA antibodies were used to quantitate protein expression levels. (**D**) Quantitation of POT1b co-localization with TRF1 at telomeres. Error bars represent standard error of the mean (s.e.m.). (**E**) Anti-Flag Western blot demonstrating that MEF cell lines used in this report expressed the indicated transgenes at approximately equal levels.

with the exception of a G to C substitution at residue 5, which almost completely abolished binding (Figure 1D). In contrast, substitutions at positions 1, 3, 4, 5 and 6 eliminated POT1a N binding to ss telomeric DNAs, a result reminiscent of the human POT1pN–ss telomeric DNA complex, where sequence specificity was greatest for nucleotides 2–5 (Figure 1C; Lei *et al*, 2004). A G to C substitution at position 10 of the telomeric substrate abolished ss telomeric DNA binding to both POT1a N and POT1b N, supporting previous results indicating that this 3′ terminal G10 residue is of critical importance for human POT1 binding to telomeres (Lei *et al*, 2004).

### *POT1b binds telomeres in vivo*

Localization of human POT1 to telomeres *in vivo* is independent of its OB-folds but does require an intact C-terminus (Loayza and de Lange, 2003; Liu *et al*, 2004a). To determine whether POT1b localizes to telomeres *in vivo*, Flag-tagged *Pot1b* cDNA constructs encoding either full-length *Pot1b*, *Pot1b* N and derivative point mutants (Figure 2A) were transiently expressed in mouse embryo fibroblasts (MEFs) at approximately equal levels (Figure 2E). Indirect immunofluorescence revealed that cells expressing full-length *Pot1b* with wild-type OB-folds displayed a punctate staining pattern, in which ~84% of POT1b containing foci co-localized with the telomere binding protein TRF1 (Figure 2B and D). In addition, full-length *Pot1b* constructs possessing either the F62A, Y89A or the Y223A point mutations also localized to telomeres. These results suggest that like mouse POT1a, functional OB-folds are not required for telomeric localization of POT1b *in vivo* (Figure 2B; Wu *et al*, 2006). Surprisingly, overexpression of *Pot1b* N in MEFs resulted in the formation of punctuate nuclear foci, ~40% of which co-localized with TRF1 (Figure 2B and D). This result suggests that POT1b can localize to telomeres *in vivo* via only its OB-folds, in marked contrast to human POT1 and mouse POT1a, which requires an intact C-terminus for telomeric localization (Loayza and de Lange, 2003; Liu *et al*, 2004a; Wu *et al*, 2006). The telomere binding specificity of the POT1b OB-folds was further confirmed by the observation that the mutant POT1b$^{Y223A}$ N protein cannot localize to telomeres *in vivo* (Figure 2B and D).

The protein TPP1 interacts with the C-terminus of POT1 to recruit it to telomeres (Houghtaling *et al*, 2004; Liu *et al*, 2004a; Ye *et al*, 2004a). To investigate whether POT1b also interacts with TPP1, we conducted co-immunoprecipitation experiments with full-length HA-tagged mouse *Tpp1* and several Flag-tagged *Pot1b* constructs. Full-length POT1b, POT1b$^{F62A}$, POT1b$^{Y89A}$ and POT1b$^{Y223A}$ mutant proteins possessing intact C-termini readily interacted with TPP1, while POT1b N did not (Figure 2C and data not shown). Direct interaction between full-length POT1b and TPP1was also detected with a yeast two-hybrid system (Table I). Finally, we demonstrate that both mouse POT1a and POT1b form a complex with TPP1 at telomeres *in vivo* (Supplementary Figure 2A and B). Taken together, these results suggest that while efficient recruitment of POT1b to telomeres *in vivo* requires an intact C-terminus, the OB-folds alone can target POT1b to telomeres.

**Table I** Two-hybrid interaction of TPP1 with POT1b WT and POT1b mutants

| | TPP1::GAL4 activation domain (AD) | PPC86::GAL4 AD |
|---|---|---|
| Pot1b FL::GAL4 DNA binding (DB) | Positive | |
| Pot1b F62A FL::GAL4 DB | Positive | |
| Pot1b N::GAL4 DB | Negative | |
| PDEST32 vector only | Negative | |
| PCL1GAL4 DB | | Positive |

Interactions are determined qualitatively by comparing intensity of β-galactosidase staining against the PCL1Gal4-PPC86 positive control.

### *MEFs expressing mutant Pot1b alleles exhibit p53-dependent senescence*

To examine the role of POT1b at telomeres, we expressed full-length wild-type *Pot1b*, *Pot1b*$^{Y89A}$ and *Pot1b*$^{Y223A}$ mutant alleles in early passage MEFs. Expression of full-length *Pot1b* in p53$^{+/+}$ MEFs minimally perturbed cellular proliferation. In contrast, overexpression of mutant *Pot1b* alleles resulted in rapid entry (within 2 days) into a phenotype resembling replicative senescence (enlarged cells with a highly vacuolated cytoplasm) that was accompanied by a four- to six-fold induction in the number of senescence-associated (SA)-β-galactosidase positive cells and an ~4-fold decline in the number of BrdU positive cells (Figure 3A and B and data not shown). This premature entry into senescence was rescued in a p53$^{-/-}$ background (Figure 3C), suggesting that it may be due to increased DNA damage initiated by the mutant *Pot1b* alleles. We noticed that p53$^{-/-}$ MEFs expressing full-length *Pot1b*$^{Y223A}$ exhibited a slower growth rate compared to cells expressing

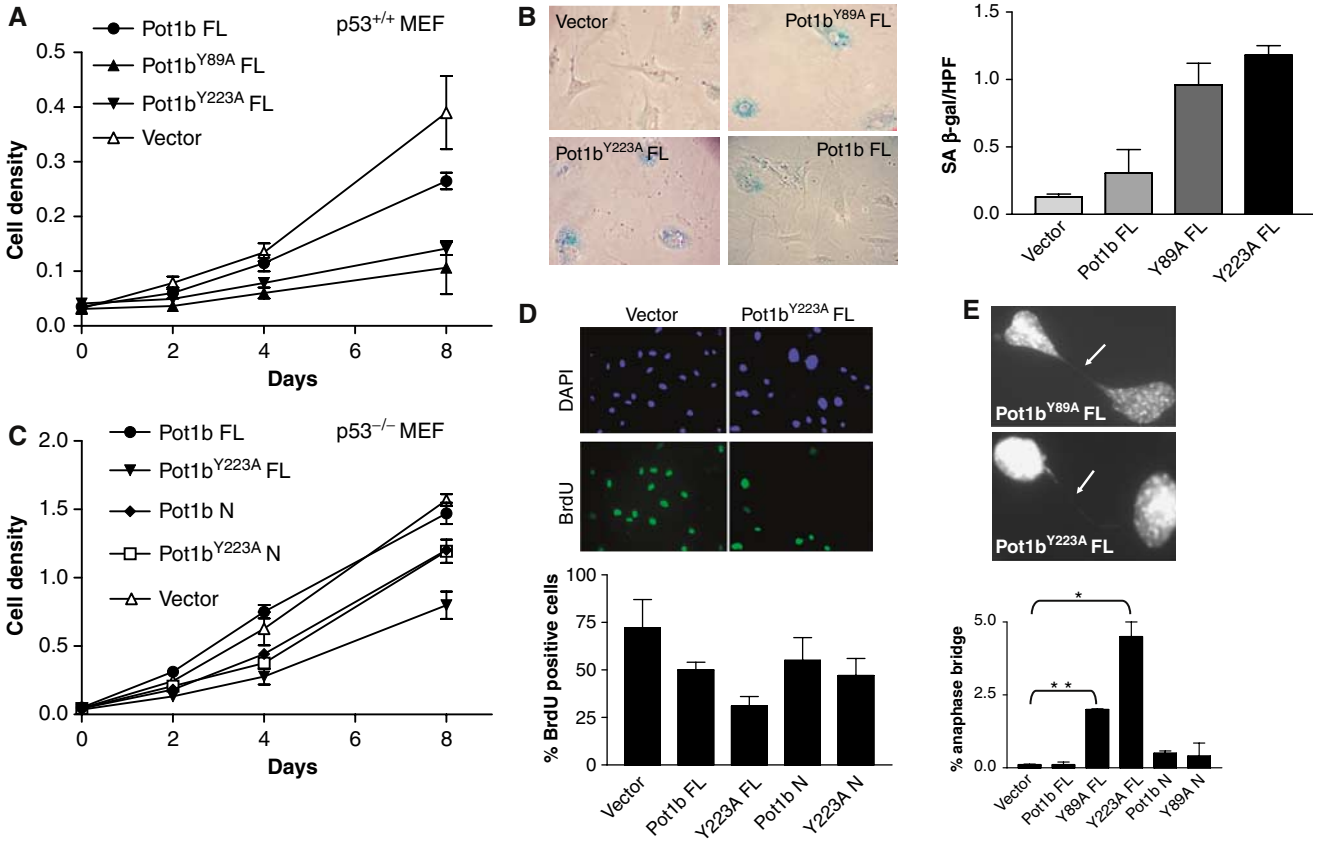


**Figure 3** Expression of mutant *Pot1b* alleles in *p53*$^{+/+}$ MEFs results in premature senescence. (**A**) Growth curve of *p53*$^{+/+}$ MEFs expressing FL *Pot1b*, FL *Pot1b*$^{Y89A}$, FL *Pot1b*$^{Y223A}$ and vector control. Error bars represent s.e.m. (**B**) Prominent SA-β-gal staining observed in MEFs expressing FL *Pot1b* mutant alleles. (**C**) Growth curve of p53$^{-/-}$ MEFs expressing the indicated constructs. Error bars represent s.e.m. (**D**) BrdU incorporation of p53$^{-/-}$ MEFs expressing indicated *Pot1b* constructs. Representative images are shown. Error bars represent s.e.m. (**E**) Elevated number of anaphase bridges (arrows) observed in *p53*$^{-/-}$ MEFs expressing FL *Pot1b*$^{Y89A}$ and FL *Pot1b*$^{Y223A}$. Anaphase bridges are expressed as a per cent of total anaphases observed. Error bars represent s.e.m. $^{*}P<0.01$; $^{**}P<0.03$.

other mutant *Pot1b* alleles, with an ~2-fold reduction in the number of BrdU positive cells (Figure 3D). This decline in cellular growth correlated with an ~15-fold increase in the number of anaphase bridges observed in DAPI-stained cells expressing full-length $Pot1b^{Y223A}$ over vector expressing controls (Figure 3E). Anaphase bridges, a hallmark of chromosomal end-to-end fusions, were also elevated in MEFs expressing full-length $Pot1b^{Y89A}$ (Figure 3E). In contrast, anaphase bridges were rare in cells expressing full-length *Pot1b*, *Pot1b* N or *Pot1b* N mutants (Figure 3E). Finally, overexpression of mutant *Pot1b* alleles did not appear to adversely influence overall telomere length (see below). Taken together, these data suggest that mutant *Pot1b* alleles perturb telomere capping function to initiate the formation of altered chromosomes, which promotes growth arrest in the setting of an intact p53 pathway.

### *Elevated DNA damage response and chromosomal aberrations in MEFs expressing full-length* $Pot1b^{Y223A}$

The induction of a phenotype resembling replicative senescence in $p53^{+/+}$ MEFs expressing mutant *Pot1b* alleles prompted us to examine whether a DNA damage response is activated at telomeres to initiate the onset of replicative senescence (d'Adda di Fagagna *et al*, 2003; Takai *et al*, 2003). Dysfunctional telomeres are detectable by the telomere dysfunction induced foci (TIF) assay that monitors telomeric association of DNA damage proteins such as γH2AX and 53BP1 (d'Adda di Fagagna *et al*, 2003; Takai *et al*, 2003; Celli and de Lange, 2005). 53BP1 associated TIFs were minimal in $p53^{-/-}$ MEFs expressing full-length *Pot1b* and $Pot1b^{Y223A}$ N (Figure 4A and B). In contrast, expression of full-length $Pot1b^{Y223A}$ and *Pot1b* N induced at least eight TIFs in ~50% and ~20% of cells examined, respectively, suggesting a robust induction of the DNA damage response at telomeres by these mutant proteins (Figure 4A and B). TIF formation was accompanied by the accumulation of other DNA damage markers, including ATM phospho-Ser 1981 and phospho-Chk2 in cells expressing full-length $Pot1b^{Y223A}$, and to a lesser extent in *Pot1b* N expressing cells (Figure 4C).

In accord with the presence of dysfunctional telomeres in cells expressing full-length $Pot1b^{Y223A}$, multiple chromosomal aberrations including p–p and p–g chromosomal arm fusions, dicentrics, fragments and rings were observed in cells expressing this mutant allele (Figure 4D; Supplementary Table 1). On average, there were 1.8 fusions per metaphase, and several cells showed tandem fusions of 4–5 chromosomes

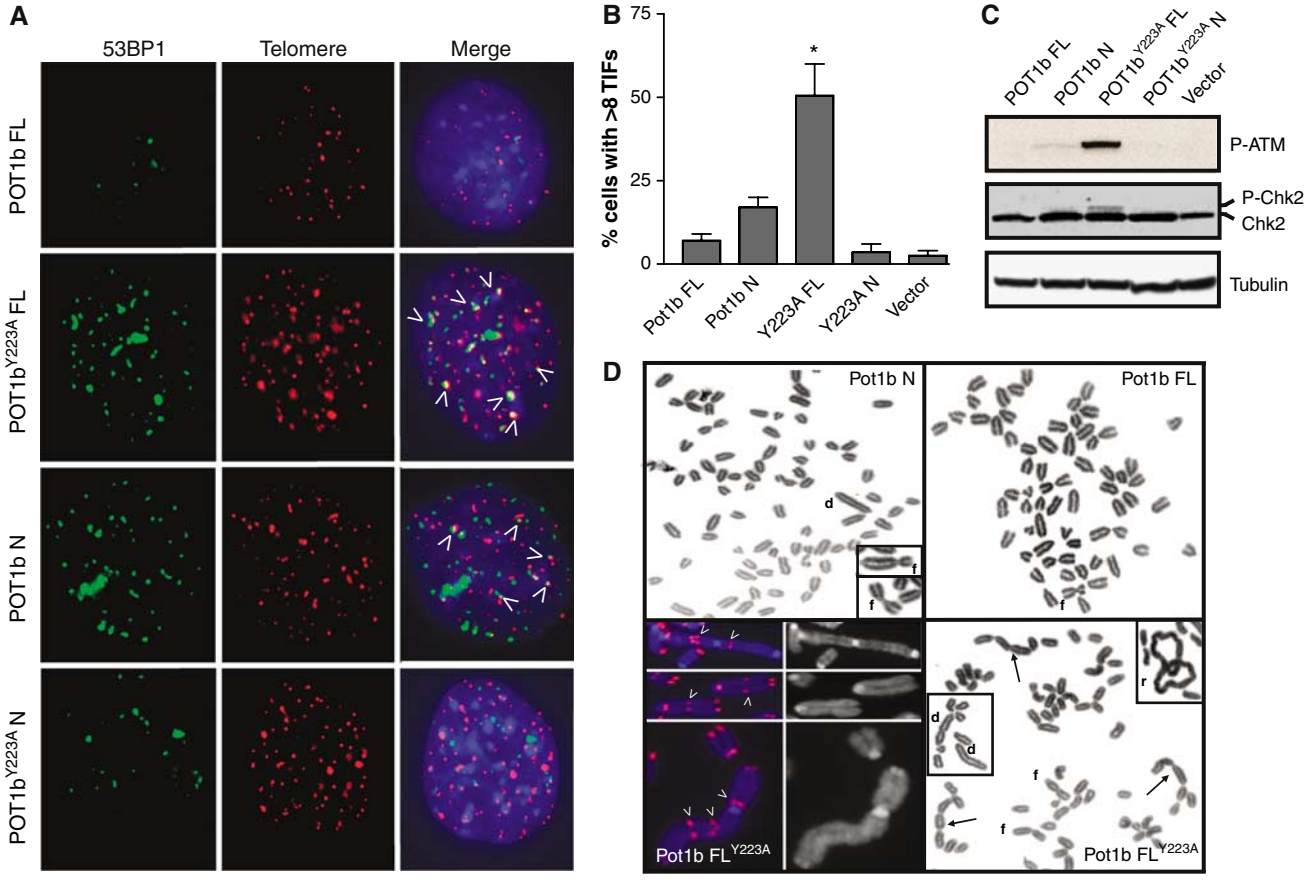


**Figure 4** Elevated DNA damage response and chromosomal aberrations in MEFs expressing mutant *Pot1b* alleles. (**A**) Co-localization of DNA damage response foci to telomeres in $p53^{-/-}$ MEFs stably expressing the indicated constructs. 53BP1 was detected with anti-53BP1 antibody (FITC, green) and telomeres were detected by telomere PNA-FISH (TRITC, red). (**B**) Quantitation of co-localization of 53BP1 with telomeres in $p53^{-/-}$ MEFs stably expressing the indicated constructs. Percentage of cells possessing >8 TIFs are indicated. A total of 100 nuclei were scored in two separate experiments. Error bars represent s.e.m. $^*P<0.01$ (Student's *t*-test). (**C**) Immunoblots detecting the phosphorylation status of ATM and Chk2 in MEF cells expressing the indicated constructs. (**D**) Chromosomal aberrations are prominent in $p53^{-/-}$ MEFs expressing FL $Pot1b^{Y223A}$ and *Pot1b* N. Arrows point to tandem chromosomal translocations, and telomere PNA-FISH characterized the majority of these fusions as possessing TTAGGG-repeats at the sites of fusion (arrowheads). r: ring chromosomes; f: p–p arm chromosomal fusions, d: dicentric chromosomes.

that were never observed in MEFs expressing full-length wild-type *Pot1b* or *Pot1b* N (Figure 4D; Supplementary Table 1). Telomere PNA FISH characterized the majority of these fusions (82%) as possessing abundant TTAGGG repeats at the site of fusion. Overexpression of *Pot1b* N also generated fused chromosomes, although at a reduced level (Figure 4D; Supplementary Figure 3 and Supplementary Table 1). These results are consistent with the notion that a subset of telomeres is rendered dysfunctional by overexpression of mutant POT1b alleles, resulting in end-to-end chromosomal fusions (Figure 4D; Supplementary Table 1).

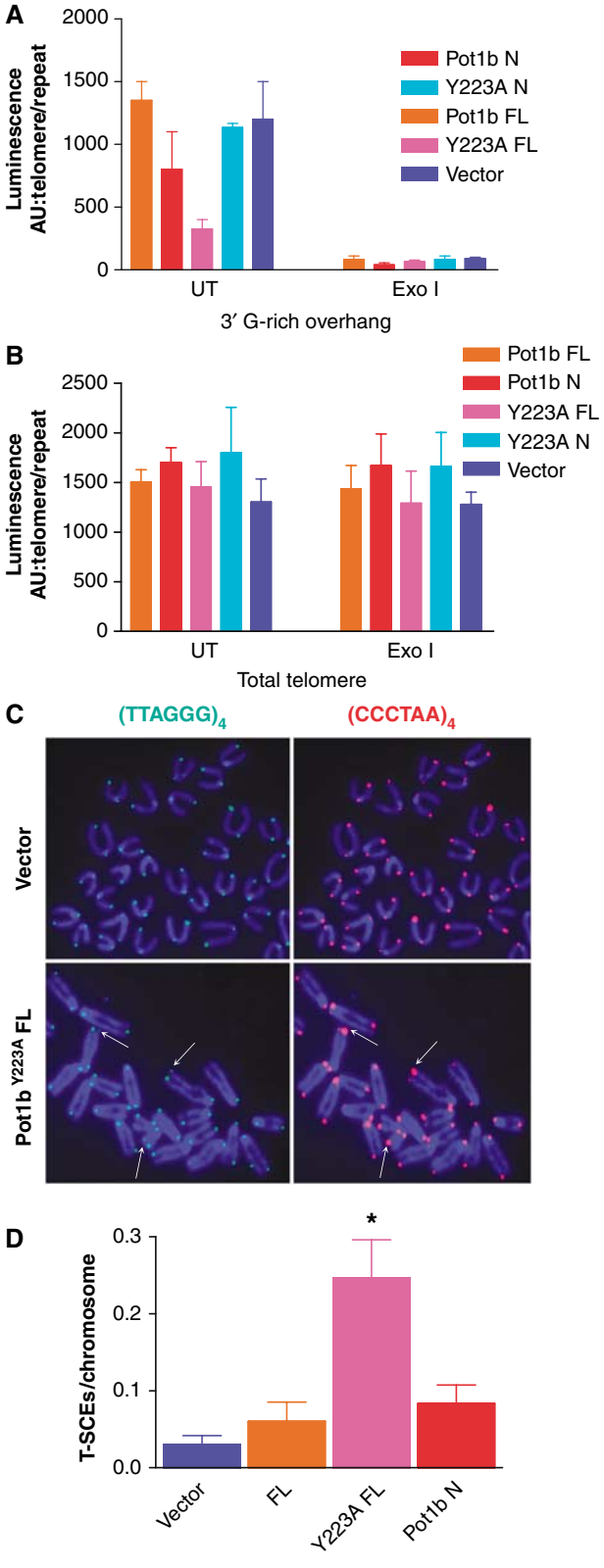


### *Reduction of 3′ G-rich telomere overhang in MEFs expressing mutant Pot1b alleles*

Previous studies have indicated that the extensive end-to-end chromosomal fusions seen in cells expressing mutant TRF2 are due to loss of the terminal 3′ G-rich overhang (van Steensel *et al*, 1998; Celli and de Lange, 2005). Since POT1b readily binds to ss telomeric DNA *in vitro*, we ascertained the status of the 3′ G-rich overhang in MEFs expressing wild-type or mutant *Pot1b* alleles. A quantitative 3′ overhang-specific hybridization protection assay (HPA) revealed that MEFs expressing full-length $Pot1b^{Y223A}$ exhibited ~60% reduction in the amount of G-rich overhang (Figure 5A; Tahara *et al*, 2005). The G-rich overhang was also slightly reduced (~18%) in MEFs expressing *Pot1b* N. In contrast, overhang length did not change appreciably in MEFs expressing full-length *Pot1b* and $Pot1b^{Y223A}$ N. The G-strand overhang was almost completely removed following treatment with Exonuclease I, demonstrating that the ss G-rich repeats originated from the 3′ end of telomeres (Figure 5A). Consistent with the robust telomeric signals detected by PNA FISH in MEFs expressing all *Pot1b* constructs (Figure 4A), HPA revealed that overall telomere length remained unchanged in cells expressing mutant *Pot1b* alleles (Figure 5B). Taken together, these results suggest that expression of full-length $Pot1b^{Y223A}$ (and to a lesser extent *Pot1b* N) resulted in a reduction of the 3′ G-overhang at telomeres, leading to telomere deprotection and end-to-end chromosomal fusions that are most likely mediated by the non-homologous end-joining (NHEJ) pathway (Smogorzewska *et al*, 2002; Celli and de Lange, 2005).

### *POT1b represses homologous recombination (HR) at telomeres*

Formation of the t-loop is postulated to prevent engagement of telomeric termini by the NHEJ pathway by sequestering the 3′ G-rich overhang. However, a t-loop resembles a Holiday junction (HJ), a structure characteristic of substrates undergoing HR. Inappropriate HR at telomeres can promote rapid deletion of telomeres, resulting in telomere shortening and premature entry into senescence (Lustig, 2003; Wang *et al*, 2004). The elevated number of chromosomal aberra-

**Figure 5** Reduction of 3′ G-rich telomere overhang and elevated T-SCEs in MEFs expressing mutant *Pot1b* alleles. (**A**) HPA using telomeric probes was performed on genomic DNA isolated from $p53^{-/-}$ MEFs (PD 4) expressing the indicated constructs to assess the length of the 3′ G-rich overhang and total telomeric DNA (**B**). UT: untreated; ExoI: genomic DNA were treated with ExoI to remove the 3′ G-rich overhang. Luminescence intensity in arbitrary units (AU) was normalized against mouse repetitive DNA A1a. (**C**) CO-FISH revealed elevated T-SCE in $p53^{-/-}$ MEFs expressing full-length $Pot1b^{Y223A}$ (arrows). Telomeres were labeled with Tam-OO-$[CCCTAA]_4$ PNA probe (red) to detect lagging strand or FITC-OO-$[TTAGGG]_4$ probe (green) to detect leading strand telomeres. (**D**) Quantification of T-SCE in $p53^{-/-}$ MEFs of the indicated genotypes. A minimum of 750 chromosomes was scored per genotype. Error bars represent s.e.m. $^*P<0.01$ (Student's *t*-test).

tions characteristic of telomere HR in *Pot1* deficient MEFs (Wu *et al*, 2006) prompted us to assess whether POT1b has a role in repressing HR at telomeres. We utilized Chromosome Orientation (CO)-FISH to assess the frequency of HR between telomeres of sister chromatids (telomere sister chromatid exchanges, T-SCEs) (Bailey *et al*, 2001). CO-FISH typically yields a characteristic pattern of two telomere signals, one on each end of the chromatid marking either lagging or leading strands, depending on the probe used for hybridization. However, a T-SCE event within telomeric DNA results in a three- (or four-) telomere hybridization signals of unequal intensity. T-SCEs were rare in MEFs expressing full-length *Pot1b* and *Pot1b* N (Figure 5C). In contrast, MEFs expressing full-length $Pot1b^{Y223A}$ exhibited ~5-fold increase in both leading- and lagging-strand T-SCE over controls (Figure 5C and D). In addition, telomere PNA FISH also detected additional cytogenetic features characteristic of aberrant telomere HR, including the presence of telomeric DNA-containing Double Minute (TDM) chromosomes (Supplementary Figure 3A and Supplementary Table 1). TDMs are proposed to result from aberrant HR events between telomeric sequences and intrachromosomal telomeric repeats (Zhu *et al*, 2003; Laud *et al*, 2005). These results suggest that POT1b plays a role in repressing aberrant HR at telomeres.

### *Both POT1a and POT1b are required to maintain chromosomal stability*

Conditional deletion of *Pot1a* results in elevated chromosomal instability and aberrant HR at telomeres (Wu *et al*, 2006). To determine whether depletion of *Pot1b* affected chromosomal stability, we utilized retroviral delivery of *Pot1b* shRNAs into MEFs. We identified two *Pot1b* shRNAs, which reduced *Pot1b* expression by >90% without affecting *Pot1a* levels (Figure 6A and data not shown). Compared to vector controls, shRNA-*Pot1b-1 and 3* depleted cells exhibited ~15-fold increase in cytogenetic aberrations, including chromosomal fusions without telomeres at the sites of fusion, isochromatid rings resulting from fusions of sister chromatids and TDMs (Figure 6B and D; Supplementary Table 1 and data not shown). Comparison of these chromosomal aberrations to those detected in MEFs expressing full-length $Pot1b^{Y223A}$ revealed that the number of fused chromosomes possessing TTAGGG repeats at the site of fusion is ~3-fold higher in MEFs expressing the mutant *Pot1b* allele (Figure 6D). Finally,

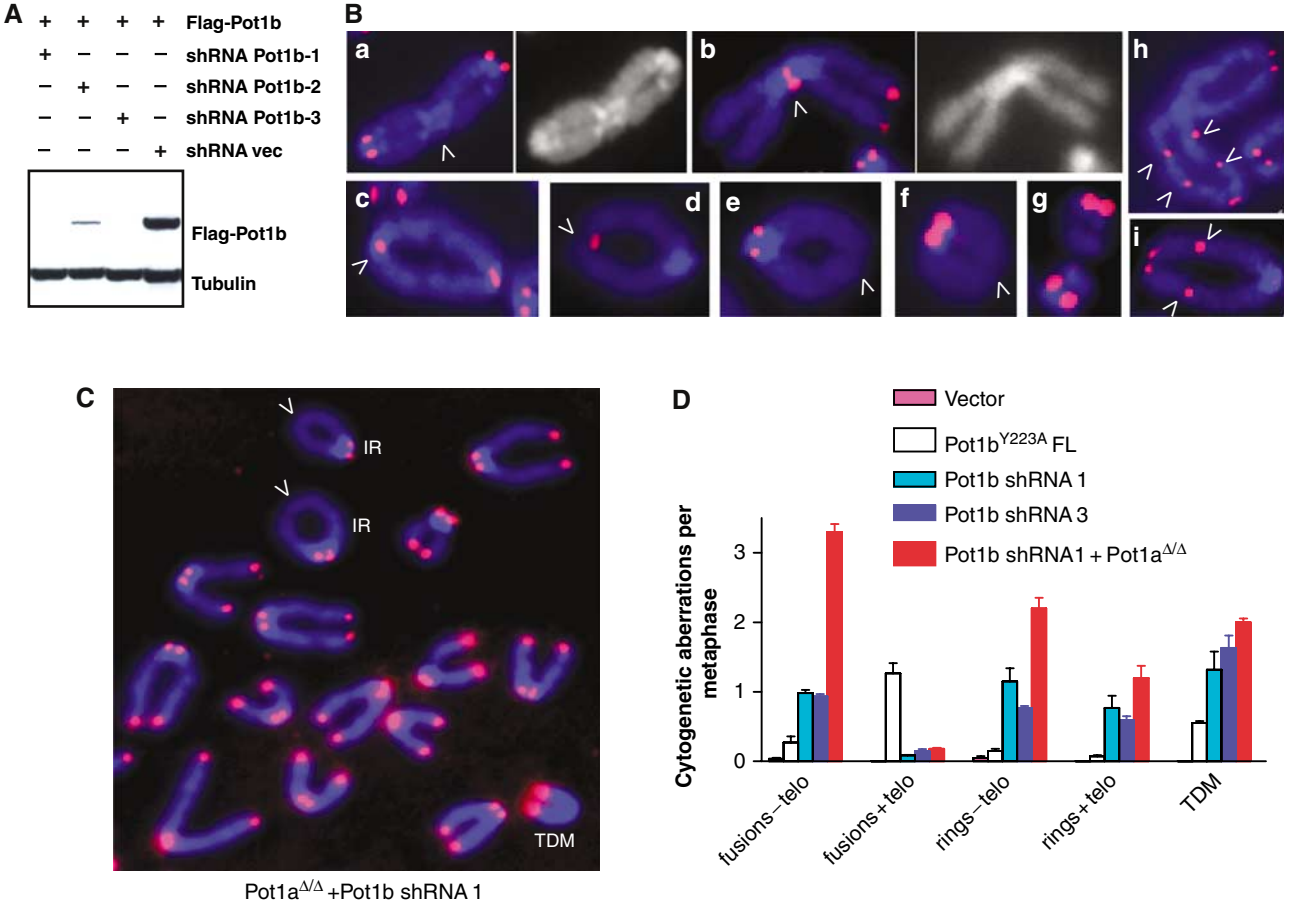


**Figure 6** Depletion of *Pot1b* results in multiple cytogenetic aberrations. (**A**) shRNA mediated knockdown of *Pot1b* in $p53^{-/-}$ MEFs. $p53^{-/-}$ MEFs expressing Flag-tagged *Pot1b* were transfected with pSUPER control (shRNA vec) or pSUPER-*Pot1b* shRNAs 1, 2 and 3 (shRNA *Pot1b* 1, 2, 3). Flag-POT1b was detected by Western. (**B**) Knockdown of *Pot1b* induced multiple chromosomal aberrations, including p–p arm fusions without TTAGGG repeats at fusion sites (a, arrowhead); p–p arm fusions with TTAGGG repeats at fusion sites (b, arrowhead); isochromatid rings with TTAGGG repeats at the sites of fusion (c, d, arrowhead indicates site of fusion); isochromatid rings without TTAGGG repeats at sites of fusion (e, f, arrowheads); TDMs (g); and dicentric chromosomes with TTAGGG repeats at multiple sites of fusion (h, j, arrowheads). (**C**) Depletion of both *Pot1* and *Pot1b* result in increased HR at telomeres. TDM: telomere double minute chromosomes, IR: isochromatid rings. (**D**) Quantification of cytogenetic aberrations of the indicated genotypes. $N = 164$ total metaphases scored. Error bars represent s.e.m.

we asked whether both POT1a and POT1b are required to maintain chromosomal stability. shRNA-*Pot1b* mediated depletion of *Pot1b* in $Pot1a^{\Delta/\Delta}$, $p53^{-/-}$ MEFs resulted in an increase in the number of TDMs (1.8 per metaphase) and isochromatid rings (3.1 per metaphase) observed over shRNA-*Pot1b* depleted MEFs (1.3 TDMs and 1.9 isochromatid rings per metaphase) and $Pot1a^{\Delta/\Delta}$, $p53^{-/-}$ MEFs (1.1 TDM and 0.45 isochromatid rings per metaphase) (Figure 6D; Wu *et al*, 2006). These results suggest that both POT1a and POT1b are required to maintain chromosomal stability.

## Discussion

The data presented here indicate that POT1b, ss telomere binding protein, plays a role in repressing both NHEJ and HR at telomeres. The presence of two POT proteins in the mouse genome suggests that they may mediate distinct roles at telomeres. Our data suggest that POT1a negatively regulates telomere length (Wu *et al*, 2006), while POT1b plays a role in maintaining the 3′ G-rich overhang.

### *Role of POT1b in telomere end protection*

Inappropriate repair of dysfunctional telomeres could adversely impact cell survival by eliciting apoptosis or cell cycle arrest in p53 competent cells (Karlseder *et al*, 1999; Celli and de Lange, 2005). Dysfunctional telomeres can be processed as double-stranded DNA breaks by the NHEJ machinery, in which Ligase IV-mediated joining of ends create fused chromosomes with TTAGGG sequences at the site of fusion (van Steensel *et al*, 1998; Smogorzewska *et al*, 2002; Celli and de Lange, 2005). NHEJ-mediated chromosomal fusions are inhibited by the presence of the 3′ G-rich overhang, and its removal promotes chromosomal end-joining (Zhu *et al*, 2003; Celli and de Lange, 2005). Repression of inappropriate NHEJ at telomeres requires formation of the telosome/shelterin complex, since deletion of specific components in this complex (TRF2 and POT1) results in NHEJ-mediated chromosomal fusions (van Steensel *et al*, 1998; Celli and de Lange, 2005; Wu *et al*, 2006). Since POT1 sequesters the terminal G10 residue of 3′ G-rich overhang into a deep binding pocket, it is predicted to be essential for telomere end protection (Lei *et al*, 2004). Additional evidence that POT1 is required for the formation of a protective telomeric structure comes from a recent study indicating that telomeres become transiently deprotected during the G2 phase of the cell cycle after partial loss of telomeric POT1 (Verdun *et al*, 2005).

Our data are consistent with the notion that a second member of the mouse POT family, POT1b, is also required for telomere end protection. POT1b preferentially binds to the 5′GGTTAGGGTTAG3′ sequence and its OB-folds are sufficient to target it to telomeres. Overexpression of mutant *Pot1b* alleles results in the activation of a robust ATM-dependent DNA damage response at telomeres that initiates a p53-dependent cell cycle arrest despite the fact that double-stranded telomeric repeats remain relatively constant. In the absence of p53, this senescent phenotype is bypassed, with elevated anaphase bridge formation and accumulation of end-to-end chromosomal fusions with TTAGGG sequence at the site of fusion. Mutant POT1b proteins might exert their effect by directly perturbing endogenous POT1b function at telomeres. For example, POT1b N could potentially compete with endogenous POT1b for access to the 3′ G-rich overhang. On the other hand, full-length $POT1b^{Y223A}$ could inhibit access of endogenous POT1b to the telosome/shelterin complex by binding TPP1. Another possibility is that overexpression of mutant POT1b alleles may disrupt POT1b's interaction with other members of the telosome/shelterin complex. The long tandemly fused chromosomes observed in cells expressing the mutant $Pot1b^{Y223A}$ allele is reminiscent of the type of chromosomal fusions observed in human cells expressing $Trf2^{\Delta B\Delta M}$ and in MEFs null for *Trf2* (van Steensel *et al*, 1998; Celli and de Lange, 2005), suggesting that full-length $POT1b^{Y223A}$ may disrupt TRF2-POT1b interaction at telomeres. While a functional interaction between TRF2 and POT1b remains to be determined, TRF2 interacts with human POT1 at telomeres (Yang *et al*, 2005).

Although POT1b represses NHEJ at telomeres, this activity is minor compared to TRF2's role in preventing NHEJ-mediated chromosomal fusions (Celli and de Lange, 2005). This result suggests that POT1b may have additional functions at telomeres. We speculate one way that cells can inhibit inappropriate NHEJ at telomeres is to adopt a t-loop structure at the ends of chromosomes to sequester the 3′ ss overhang. However, a t-loop also resembles a HR substrate. In normal cells, inappropriate HR at telomeres must be repressed, since branch migration of the 3′ overhang in a t-loop can create an HJ that can be cleaved by HJ resolvase to initiate telomere deletion (Lustig, 2003; Wang *et al*, 2004). Recently, we demonstrated that POT1a plays a role in repressing inappropriate HR at telomeres (Wu *et al*, 2006). In cells deficient in *Pot1a*, multiple chromosomal aberrations characteristic of telomere HR were present. Here, we extend this observation to POT1b, and show that shRNA-mediated depletion of *Pot1b* also resulted in elevated telomere HR. Cytogenetic abnormalities characteristic of telomere HR, including TDMs, isochromatid rings and elevated T-SCEs are elevated in *Pot1b* depleted cells and in cells expressing mutant *Pot1b* alleles. In addition, depletion of both *Pot1a* and *Pot1b* led to increased chromosomal aberrations, suggesting that both POT proteins are required to repress inappropriate NHEJ and HR at telomeres.

### *Separation of function in mouse POT proteins*

The observation that there are two POT proteins encoded by the mouse genome while there is only one in human suggests that mouse POT proteins may perform separate functions at telomeres. This notion is supported from recent data indicating that *Arabidopsis* has two POT1-like proteins, one which is involved in telomere length regulation and the other involved in chromosome end protection (Shakirov *et al*, 2005). We recently demonstrated that mouse POT1a is required for telomere length homeostasis, since conditional deletion of *Pot1a* in MEFs resulted in telomere length elongation. In addition, deletion of *Pot1a* correlated with an increase in the 3′ G-rich overhang, suggesting that it may regulate a C-strand nuclease (Wu *et al*, 2006). In contrast, data presented here suggest that POT1b is required for maintenance of the 3′ G-rich overhang and has no appreciable role in telomere length regulation. Both proteins are required to repress NHEJ and telomere HR. Taken together, these results suggest that the two mouse POT proteins may have both distinct and overlapping functions in mediating telomere end protection. This observation is interesting in light of a recent

 

report suggesting that telomeres exist in extendible and non extendible states, and that telomerase acts preferentially on the shortest telomeres (Teixeira *et al*, 2004). POT1a may negatively regulate telomere length by inhibiting telomerase access to the terminal G-residue in long telomeric substrates while promoting telomere extension by enabling telomerase to access short telomeric ends (Kelleher *et al*, 2005; Lei *et al*, 2005). POT1b would serve to protect the unfolded 3′ overhang from exposure to degrading nucleases, and given that its OB-folds can directly bind to telomeres *in vivo*, it is possible that this end protective function may not require other components of the telosome. It will be of interest to determine whether subcomplexes containing varying ratios of the POT proteins exist on telomeres at different phases of the cell cycle to modulate telomere elongation and protection.

## Materials and methods

### *Cloning of murine Pot1b, site-directed mutagenesis and expression analysis*

Based on cDNA XM_355022, we used a PCR strategy to clone mouse *Pot1b* cDNA in frame with a 5′ Flag epitope tag, inserted it into the KS plasmid (Stratagene) and fully sequenced. *Pot1b* deletion constructs were generated by PCR and the sequenced inserts subcloned into pcDNA3.1 (Clonetech) and pQCXIP (Novex) vectors. N-terminal POT1b consisted of aa 1–341. Site-directed mutagenesis was performed according to the manufacturer's instructions (Strategene), in which phenylalanine at position 62 and tyrosine at position 89 and tyrosine at position 223 were individually mutated into alanines. First-strand cDNA panels (Clontech) were used to detect *Pot1b* expression. Transcripts were amplified using AdvanTaq 2 PCR Kit (Clontech) and *G3PDH* was amplified under the same conditions following manufacturer's recommendations.

### *Cell culture, immunolocalization studies and microscopy*

$p53^{+/+}$ and $p53^{-/-}$ MEFs (passage 1–3) and 293 T cells were maintained in Dulbecco's modified Eagle's medium and cultured at 3% oxygen to minimize premature entry into senescence (Parrinello *et al*, 2003). For immunolocalization studies, *Pot1b* constructs subcloned in the retroviral vector pQCXIP were infected into rapidly growing early passage MEFs, either wild type or null for p53. Infected cells were plated onto eight-well chambers and harvested 24–48 h after infection. Immunofluorescence was performed as described (Laud *et al*, 2005) and POT1b was localized with anti-Flag antibody (Sigma) at 1:10 000. Polyclonal antibody against mTRF1 (a generous gift from Jan Karlseder, Salk Institute) was used at 1:2000. Images were acquired on a Nikon Eclipse 800 with $\times 63$ and $\times 100$ plan-apo objectives and photographed with a cooled CCD camera. CCD chip nonlinearities were removed by taking bias and dark current frames and the optical train flat fielded to eliminate vignetting. Individual raw images were taken through DAPI, Rhodamine and FITC narrowband filters and stacked in MetaMorph and PhotoShop CS were utilized to compose the final images. The same amount of linear histogram stretch was applied to all raw images before stacking to maintain the same degree of contrast enhancement in all images.

### *In vitro translation, gel shift and immunoprecipitation assays*

*Pot1b* constructs under the control of the T7 expression vector were translated *in vitro* with the TNT coupled reticulocyte lysate kit (Promega) under the manufacturer's recommended conditions. DNA binding assays were performed essentially as described (Baumann *et al*, 2002) and fractionated at 4°C on a 4–20% polyacrylamide Tris–borate EDTA gel. The gels were dried, and radiolabeled ssDNA was visualized by exposure to a PhosphorImager. To determine the interaction between mouse POT1b and TPP1, we cloned the *Tpp1* cDNA based on cDNA gi:22823923 (Liu *et al*, 2004a), in frame with a 5′ HA epitope tag and verified the construct by sequencing. Various Flag-tagged *Pot1b* constructs and full-length HA-*Tpp1* were co-transfected into 293T cells, and IP performed as described (Ye *et al*, 2004a).

### *Yeast two-hybrid analysis*

Yeast two-hybrid was performed using Proquest Two-Hybrid System with Gateway Technology (Invitrogen), according to the manufacturer's protocol. Mouse *Tpp1* was cloned into pDESt22 to generate a fusion protein with the yeast GAL4 activation domain, while full-length *Pot1b*, full-length $Pot1b^{F62A}$ and *Pot1b* N constructs were cloned into pDEST32 to generate a fusion protein with the GAL4 DNA binding domain using Gateway LR Recombination Systems (Invitrogen). Proteins interactions were tested using β-Gal Filter Assay, as described (Wu *et al*, 2006).

### *Western blot analysis, growth analysis, SA β-gal assay and anaphase bridge determination*

The antibodies used for Western analyses were phospho-ATM Ser 1981 (Cell Signalling; 1:1000) and Chk2 (BD Biosciences, 1: 500). Anti-mouse γ-tubulin (Sigma, 1:10 000) was used as a loading control. For growth curves, $4 \times 10^4$ stably infected MEFs were plated in triplicate into six-well plates. At 0, 2, 4, 8 days post plating, cells were fixed and stained with crystal violet. SA β-gal assay was performed as described (Dimri *et al*, 1995). BrdU incorporation was performed essentially as described (Smogorzewska *et al*, 2002). Anaphase bridges were quantitated from a minimum of 200 metaphase plates undergoing anaphase and determining percentage possessing a distinct chromatin bridge after DAPI staining.

### *G-tail HPA*

HPA was performed as described (Tahara *et al*, 2005) and 1 μg non-denatured genomic DNA and 0.5 μg heat-denatured genomic DNA was used per assay for the detection of telomere 3′ overhangs and total telomere DNA, respectively. To check specificity of G-tail detection, non-denatured genomic DNA was treated with Exonuclease I (30 U/μg DNA) at 37°C overnight, and heat inactivated at 80°C for 20 min, before G-tails were assayed.

### *CO-FISH analysis for T-SCEs*

CO-FISH has been described in detail previously (Bailey *et al*, 2001). Hybridization of metaphase spreads was performed with TRITC-OO-$(TTAGGG)_4$ or FITC-OO-$(CCCTAA)_4$ peptide nucleic acid probes (Applied Biosystems). For simultaneous visualization of both leading and lagging strands, both probes were used at a concentration of 0.5 μg/ml. For CO-FISH, a minimum of 750 chromosome ends were scored blinded for each genotype, and pairwise comparisons for statistical significance were made by Student's *t*-test. Differences between genetic backgrounds are considered significant only when *P*-values were less than 0.01. Images were captured with Metamorph Premiere (Molecular Devices) and processed with Metamorph and Adobe Photoshop CS.

### *shRNA interference*

Three shRNA-*Pot1b* were generated in pSuper as described (Deng *et al*, 2003). To generate pRetro-Super constructs, *Eco*R1- and *Xho*I-digested insert from pSuper was subcloned into the same site into pRetro-Super vector (Brummelkamp *et al*, 2002). The target sequence for mouse *Pot1b* is: shRNA–Pot1b-1: position 372 to 390 (5′CTTCACTGCTCAGGAC TAC3′); shRNA-Pot1b-2: position 623641 (5′GTCACATTCTGCAGCTACA3′); shRNA–Pot1b-3: position 962–980 (5′GCTCTGAATCAGACCTAGT3′)

### *Note added in proof:*

Cloning and characterization of Pot1b was recently reported by Hockemeyer *et al* (2006) *Cell* **126:** 63–77.

## Acknowledgements

We are grateful to Jan Karlseder for providing TRF1 antibody, and Philip Carpenter for the 53BP1 antibody. We acknowledge the TC Hsu Molecular Cytogenetics Core for outstanding cytogenetic services (NCI No. CA016672). We thank members of the Chang lab for helpful comments. SC acknowledges generous financial support from the Welch Foundation, the Elsa U Pardee Foundation, the Sidney Kimmel Foundation for Cancer Research, the Abraham and Phyllis Katz Foundation, and the Michael Kadoorie Cancer Genetic Research Program.

## References

Bailey SM, Cornforth MN, Kurimasa A, Chen DJ, Goodwin EH (2001) Strand-specific postreplicative processing of mammalian telomeres. *Science* **293:** 2462–2465

Baumann P, Cech TR (2001) Pot1, the putative telomere end-binding protein in fission yeast and humans. *Science* **292:** 1171–1175

Baumann P, Podell E, Cech TR (2002) Human Pot1 (protection of telomeres) protein: cytolocalization, gene structure, and alternative splicing. *Mol Cell Biol* **22:** 8079–8087

Brummelkamp TR, Bernards R, Agami R (2002) A system for stable expression of short interfering RNAs in mammalian cells. *Science* **296:** 550–553

Celli GB, de Lange T (2005) DNA processing is not required for ATM-mediated telomere damage response after TRF2 deletion. *Nat Cell Biol* **7:** 710–712

Chandra A, Hughes TR, Nugent CI, Lundblad V (2001) Cdc13 both positively and negatively regulates telomere replication. *Genes Dev* **15:** 404–414

de Lange T (2005) Shelterin: the protein complex that shapes and safeguards human telomeres. *Genes Dev* **19:** 2100–2110

d'Adda di Fagagna FD, Reaper PM, Clay-Farrace L, Fiegler H, Carr P, von Zglinicki T, Saretzki G, Carter NP, Jackson SP (2003) A DNA damage checkpoint response in telomere-initiated senescence. *Nature* **426:** 194–198

Deng Y, Ren X, Yang L, Lin Y, Wu X (2003) A JNK-dependent pathway is required for TNFalpha-induced apoptosis. *Cell* **115:** 61–70

Dimri GP, Lee XH, Basile G, Acosta M, Scott C, Roskelley C, Medrano EE, Linskens M, Rubelj I, Pereirasmith O, Peacocke M, Campisi J (1995) A biomarker that identifies senescent human-cells in culture and in aging skin *in-vivo*. *Proc Natl Acad Sci USA* **92:** 9363–9367

Garvik B, Carson M, Hartwell L (1996) Single-stranded DNA arising at telomeres in cdc13 mutants may constitute a specific signal for the RAD9 checkpoint. *Mol Cell Biol* **15:** 6128–6138

Griffith JD, Comeau L, Rosenfield S, Stansel RM, Bianchi A, Moss H, de Lange T (1999) Mammalian telomeres end in a large duplex loop. *Cell* **97:** 503–514

Hemann MT, Greider CW (1999) G-strand overhangs on telomeres in telomerase-deficient mouse cells. *Nucl Acids Res* **27:** 3964–3969

Hockemeyer D, Daniels JP, Takai H, de Lange T (2006) Recent expansion of the telomeric complex in rodents: two distinct POT1 proteins protect mouse telomeres. *Cell* **126:** 63–77

Horvath MP, Schweiker VL, Bevilacqua JM, Ruggles JA, Schultz SC (1998) Crystal structure of the *Oxytricha nova* telomere end binding protein complexed with single strand DNA. *Cell* **95:** 963–974

Houghtaling BR, Cuttonaro L, Chang W, Smith S (2004) A dynamic molecular link between the telomere length regulator TRF1 and the chromosome end protector TRF2. *Curr Biol* **14:** 1621–1631

Karlseder J, Broccoli D, Dai Y, Hardy S, De Lange T (1999) p53- and ATM-dependent apoptosis induced by telomeres lacking TRF2. *Science* **283:** 1321–1325

Kelleher C, Kurth I, Lingner J (2005) Human protection of telomeres 1 (POT1) is a negative regulator of telomerase activity *in vitro*. *Mol Cell Biol* **25:** 808–818

Kim S, Beausejour C, Davalos AR, Kaminker P, Heo SJ, Campisi J (2004) TIN2 mediates functions of TRF2 at human telomeres. *J Biol Chem* **279:** 43799–43804

Laud PR, Multani AS, Bailey SM, Wu L, Ma J, Kingsley C, Lebel M, PathakS, DePinho RA, Chang S (2005) Elevated telomere–telomere recombination in WRN-deficient, telomere dysfunctional cells promotes escape from senescence and engagement of the ALT pathway. *Genes Dev* **19:** 2560–2570

Lei M, Baumann P, Cech TR (2002) Cooperative binding of single-stranded telomeric DNA by the Pot1 protein of *Schizosaccharomyces pombe*. *Biochemistry* **41:** 14560–14568

Lei M, Podell ER, Baumann P, Cech TR (2003) DNA self-recognition in the structure of Pot1 bound to telomeric single-stranded DNA. *Nature* **426:** 198–203

Lei M, Podell ER, Cech TR (2004) Structure of human POT1 bound to telomeric single-stranded DNA provides a model for chromosome end-protection. *Nat Struct Mol Biol* **11:** 1223–1229

Lei M, Zaug AJ, Podell ER, Cech TR (2005) Switching human telomerase on and off with hPOT1 protein *in vitro*. *J Biol Chem* **280:** 20449–20456

Liu D, O'Connor MS, Qin J, Songyang Z (2004b) Telosome, a mammalian telomere-associated complex formed by multiple telomeric proteins. *J Biol Chem* **279:** 51338–51342

Liu D, Safari A, O'Connor MS, Chan DW, Laegeler A, Qin J, Songyang Z (2004a) PTOP interacts with POT1 and regulates its localization to telomeres. *Nat Cell Biol* **6:** 673–680

Loayza D, de Lange T (2003) POT1 as a terminal transducer of TRF1 telomere length control. *Nature* **423:** 1013–1018

Loayza D, Parsons H, Donigian J, Hoke K, de Lange T (2004) DNA binding features of human POT1: a nonamer 5′-TAGGGTTAG-3′ minimal binding site, sequence specificity, and internal binding to multimeric sites. *J Biol Chem* **279:** 13241–13248

Lustig AJ (2003) Clues to catastrophic telomere loss in mammals from yeast telomere rapid deletion. *Nat Rev Genet* **4** (11)**:** 916–923

Mitton-Fry RM, Anderson EM, Hughes TR, Lundblad V, Wuttke DS (2002) Conserved structure for single-stranded telomeric DNA recognition. *Science* **96:** 145–147

Murti KG, Prescott DM (1999) Telomeres of polytene chromosomes in a ciliated protozoan terminate in duplex DNA loops. *Proc Natl Acad Sci USA* **96:** 14436–14439

Nikitina T, Woodcock CL (2004) Closed chromatin loops at the ends of chromosomes. *J Cell Biol* **166:** 161–165

Parrinello S, Samper E, Krtolica A, Goldstein J, Melov S, Campisi J (2003) Oxygen sensitivity severely limits the replicative lifespan of murine fibroblasts. *Nat Cell Biol* **5:** 741–747

Price CM, Cech TR (1987) Telomeric DNA–protein interactions of *Oxytricha* macronuclear DNA. *Genes Dev* **1:** 783–793

Shakirov EV, Surovtseva YV, Osbun N, Shippen DE (2005) The *Arabidopsis* Pot1 and Pot1b proteins function in telomere length homeostasis and chromosome end protection. *Mol Cell Biol* **25:** 7725–7733

Smogorzewska A, Karlseder J, Holtgreve-Grez H, Jauch A, de Lange T (2002) DNA ligase IV-dependent NHEJ of deprotected mammalian telomeres in G1 and G2. *Curr Biol* **12:** 1635–1644

Tahara H, Kusunoki M, Yamanaka Y, Matsumura S, Ide T (2005) G-tail telomere HPA: simple measurement of human single-stranded telomeric overhangs. *Nat Methods* **2:** 829–831

Takai H, Smogorzewska A, de Lange T (2003) DNA damage foci at dysfunctional telomeres. *Curr Biol* **13:** 1549–1556

Teixeira MT, Arneric M, Sperisen P, Lingner J (2004) Telomere length homeostasis is achieved via a switch between telomerase-extendible and -nonextendible states. *Cell* **117:** 323–335

Trujillo KM, Bunch JT, Baumann P (2005) Extended DNA binding site in Pot1 broadens sequence specificity to allow recognition of heterogeneous fission yeast telomeres. *J Biol Chem* **280:** 9119–9128

van Steensel B, Smogorzewska A, De Lange T (1998) TRF2 protects human telomeres from end-to-end fusions. *Cell* **92:** 401–413

Verdun RE, Crabbe L, Haggblom C, Karlseder J (2005) Functional human telomeres are recognized as DNA damage in G2 of the cell cycle. *Mol Cell* **20:** 551–561

Wang RC, Smogorzewska A, de Lange T (2004) Homologous recombination generates T-loop-sized deletions at human telomeres. *Cell* **119:** 355–368

Wei C, Price CM (2004) Cell cycle localization, dimerization, and binding domain architecture of the telomere protein cPot1. *Mol Cell Biol* **24:** 2091–2102

Wong KK, Chang S, Depinho RA (2006) Modeling cancer and aging in the telomerase-deficient mouse. In *Telomeres*, de Lange T, Lundblad V, Blackburn E (eds), pp 109–138. Cold Spring Harbor: Cold Spring Harbor Laboratory Press

Wu L, Multani AS, He H, Cosme-Blanco W, Deng Y, Deng JM, Bachilo O, Pathak S, Tahara H, Bailey SM, Deng Y, Behringer RR, Chang S (2006) *Pot1* deficiency initiates DNA damage checkpoint activation and aberrant homologous recombination at telomeres. *Cell* **126:** 49–62

Yang Q, Zheng YL, Harris CC (2005) POT1 and TRF2 cooperate to maintain telomeric integrity. *Mol Cell Biol* **25:** 1070–1080

Ye JZ, Donigian JR, van Overbeek M, Loayza D, Luo Y, Krutchinsky AN, Chait BT, de Lange T (2004b) TIN2 binds TRF1 and TRF2 simultaneously and stabilizes the TRF2 complex on telomeres. *J Biol Chem* **279:** 47264–47271

Ye JZ, Hockemeyer D, Krutchinsky AN, Loayza D, Hooper SM, Chait BT, de Lange T (2004a) POT1-interacting protein PIP1: a telomere length regulator that recruits POT1 to the TIN2/TRF1 complex. *Genes Dev* **18:** 1649–1654

Zhu XD, Niedernhofer L, Kuster B, Mann M, Hoeijmakers JH, de Lange T (2003) ERCC1/XPF removes the 3′ overhang from uncapped telomeres and represses formation of telomeric DNA-containing double minute chromosomes. *Mol Cell* **12:** 1489–1498

 